minerals

MDPI

Article

The Effects of Hydrochloric Acid Pretreatment on Different Types of Clay Minerals

Bin Hu [1,2,3], Chunxia Zhang [1,2,4,*] and Xiaoyan Zhang [1,2,4]

[1] Key Laboratory of Cenozoic Geology and Environment, Institute of Geology and Geophysics, Chinese Academy of Sciences, Beijing 100029, China
[2] Institution of Earth Science, Chinese Academy of Science, Beijing 100029, China
[3] College of Earth and Planetary Sciences, University of Chinese Academy of Sciences, Beijing 100049, China
[4] College of Earth Science and Engineering, Shandong University of Science and Technology, Qingdao 266590, China
* Correspondence: cxzhang@mail.iggcas.ac.cn

Abstract: Clay minerals are common in geological samples and are useful paleoclimate and sediment provenance proxies. Acid pretreatment is the most common method for the separation and purification of clay minerals. Given that hydrochloric acid (HCl) can dissolve chlorite and distinguish it from kaolinite, the HCl digestion method is used to simplify the routine method of clay mineral analysis. However, there have been few studies of the effects of acid digestion on different clay minerals in the context of extracting paleoclimate indicators. In this study, we used illite, chlorite, kaolinite, and two types of smectite to assess the effects of pretreatment with different HCl concentrations at variable temperatures. Our results show that chlorite is the most soluble clay mineral in HCl and can be effectively dissolved in HCl with concentrations of >1 N. The variable crystal structure of smectite affects its solubility in HCl. Ca-rich smectite, which has more cation substitution of octahedral Al, can be dissolved with HCl. However, Na-rich smectite, which has less cation substitution for octahedral Al, is hardly dissolved in HCl of any concentration or at any temperature. Illite can be partly dissolved in HCl, and the threshold beyond which dissolution occurs is 5 N HCl at 70 °C. Kaolinite is relatively difficult to dissolve in HCl. Given that the HCl digestion method uses the peak intensity of the bulk sample X-ray diffraction (XRD) analysis, whereas the routine method uses the peak area of clay particles, we compared the results of clay mineral quantification and the paleoclimate proxy obtained using the two methods for synthetically prepared mixed and natural clay samples. The results obtained with the HCl digestion method are less accurate than those obtained with the routine method because of the dissolution of illite and smectite in HCl. Therefore, the HCl pretreatment method is not suitable for clay mineral analysis in paleoclimate studies. The present results provide reference data for future studies that employ the acid dissolution pretreatment of clay mineral samples to acquire and quantify paleoclimate proxies.

Keywords: hydrochloric acid pretreatment; clay mineralogy; X-ray diffraction

Citation: Hu, B.; Zhang, C.; Zhang, X. The Effects of Hydrochloric Acid Pretreatment on Different Types of Clay Minerals. *Minerals* **2022**, *12*, 1167. https://doi.org/10.3390/min12091167

Academic Editor: Emanuela Schingaro

Received: 9 August 2022
Accepted: 12 September 2022
Published: 15 September 2022

1. Introduction

Clay minerals can be used in studies of sediment provenance, paleoclimate, tectonism, and glacio-eustasy. They are widely investigated in geological studies and even in the context of extraterrestrial asteroids and planets [1–5].

Paleoclimate reconstructions based on clay mineralogy require accurate identification and quantification during clay mineral analysis [2,6]. X-ray diffraction (XRD) is the most widely used method in this regard, although other techniques such as Fourier transform infrared spectroscopy (FTIR), chemical analysis, and electron microscopy are also used [7]. The routine method of clay mineral analysis by XRD involves first enriching the

clay particles by removing the cement components (Fe oxides, organic matter, and carbonate minerals). The second step is dispersing the clays into a liquid suspension, which is followed by water flotation [8]. The extracted clay fraction (usually <2 μm) is then smeared on glass slides with different cations and organic molecule saturations, subjected to different heating conditions, and analysed [2,8]. Given that thousands of samples need to be analysed in a paleoclimate research study, the routine method is time-consuming. Some studies of clay minerals in sedimentary sequences have simplified the routine method by using the bulk sample instead of the clay fraction for the XRD analysis [9]. Hydrochloric acid (HCl) pretreatment can be used to distinguish chlorite from kaolinite [9]. However, the conditions under which chlorite can be efficiently removed with minimum damage to the other clay minerals remain to be identified. Differences in the results between the HCl pretreatment and routine methods also need to be evaluated.

In paleoclimatic and paleoenvironmental reconstructions, numerous geochemical, physical, biological, and mineralogical proxies can be used, including clay mineral assemblage [10–12]. Acid pretreatment is commonly used for separation and purification prior to the acquisition of paleoclimate proxy data. This includes grain size analysis where acid is used to remove carbonate cement, the determination of the chemical index of weathering where acid is used to dissolve secondary minerals, the quantification of Fe speciation where acid is used for the sequential extraction of different Fe phases, and the O isotope analysis of single minerals where acid is used to purify the target mineral [13–18]. Acid dissolution of the common clay minerals is relevant to the use of clay minerals in a variety of paleoclimate studies. Previous studies have described the surface properties and behaviours of clay minerals after acid pretreatment [19–22]. However, there have been few studies of the effects of acid pretreatment on the different clay minerals used to extract paleoclimate indicators.

In this study, we analysed kaolinite, chlorite, illite, and smectite in the samples as common clay minerals in geological materials. We determined the stability of the crystal structures of clay minerals in different HCl concentrations and at variable temperatures using XRD, transmission electron microscopy (TEM), and elemental analysis. We also evaluated the differences in quantitative clay mineral analysis results between the HCl pretreatment and routine methods, based on analysis of synthetically prepared mixed-clay standards and natural samples. Our data provide insights into the analysis of clay minerals and their use in paleoclimate studies where HCl pretreatment is utilized.

2. Materials and Methods

2.1. Samples Description

We selected five clay minerals (kaolinite, chlorite, illite, Na-rich smectite, and Ca-rich smectite) to assess the effects of HCl under different experimental conditions. The clay samples were purchased from Zhejiang Sanding Technology. The sample of kaolinite is relatively pure. The samples of two types smectite were Ca-rich smectite with more cation substitution of octahedral Al (hereinafter referred to as Ca-smectite) and Na-rich smectite with less cation substitution for octahedral Al (hereinafter referred as Na-smectite), and the only accessory mineral in the Na- and Ca-rich smectites is quartz (<5%). The sample of chlorite contains 40% chlorite and 60% talc. The sample of illite contains 75% illite, 25% quartz, and traces of anatase (<1%) (Figure 1). Chemical analysis of the five samples was undertaken by X-ray fluorescence (XRF) spectrometry with a Philips PW2404 XRF spectrometer in the Analytical Laboratory of the Beijing Research Institute of Uranium Geology, Beijing, China (Table S1 [23]). The structural formulae of these five clay minerals are estimated to be as follows: kaolinite = $Al_4Si_4O_{10}(OH)_8$, Na-smectite = $(Na_{0.58}, Ca_{0.02})(Al_{1.40}, Mg_{0.32}, Fe^{3+}_{0.09}, Fe^{2+}_{0.01})Si_4O_{10}(OH)_2$, Ca-smectite = $(Ca_{0.2})(Al_{1.17}, Mg_{0.62}, Fe^{3+}_{0.12}, Fe^{2+}_{0.02}, Ti_{0.01})(Si_{3.97}, Al_{0.03})O_{10}(OH)_2$, chlorite = $(Fe_{0.33}, Mg_{3.12}, Al_{0.55})(Si_{3.35}, Al_{0.65})O_{10}(OH)_8$, and illite = $(K_{0.30,}\, Na_{0.06}, Ca_{0.01})(Al_{1.87}, Mg_{0.05}, Fe^{3+}_{0.03}, Fe^{2+}_{0.01}, Ti_{0.05})Si_4O_{10}(OH)_2$.

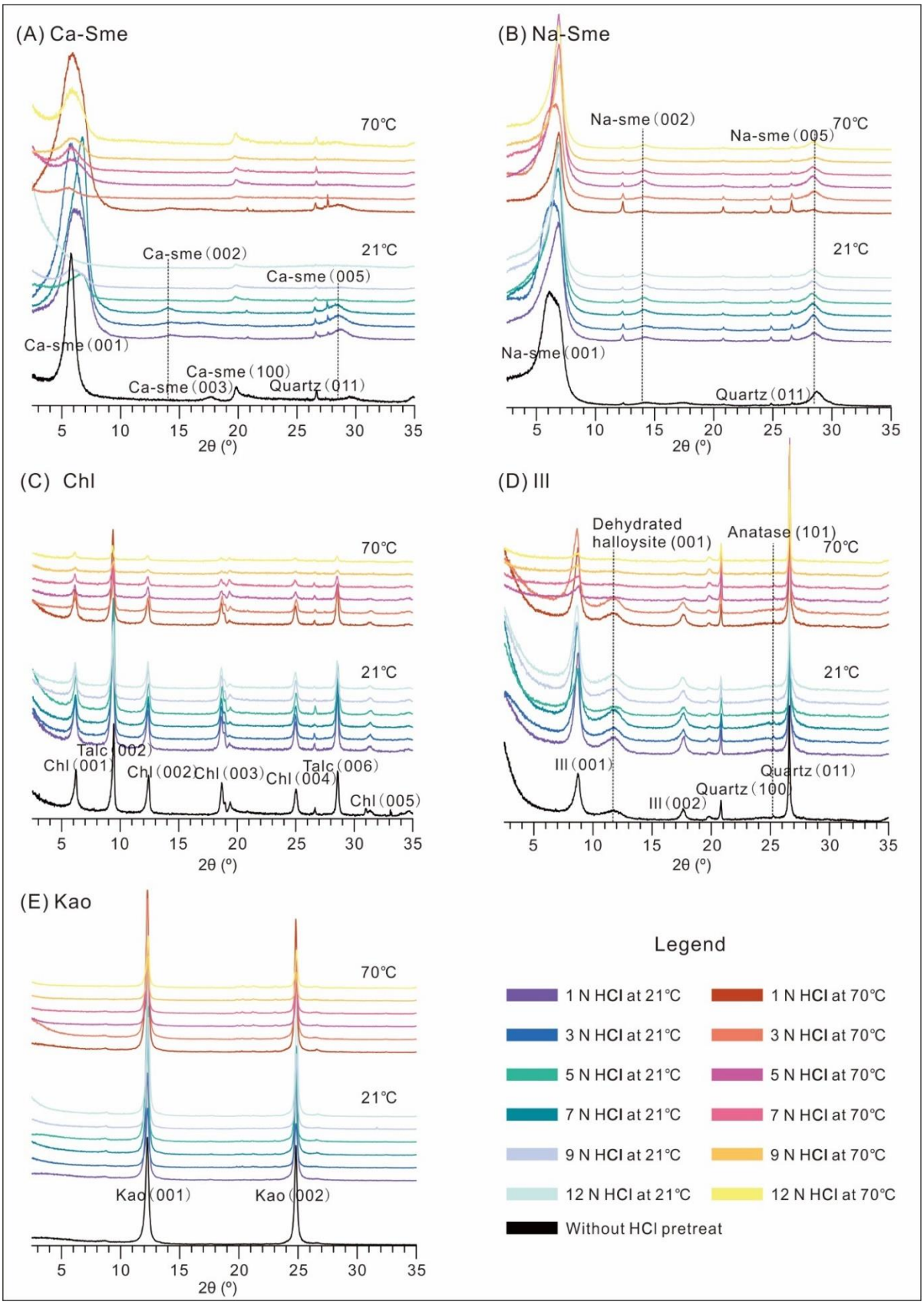

Figure 1. X-ray diffraction (XRD) patterns of the individual clay mineral samples after different pre-treatments with HCl. Black curves are the original standard samples; dark blue curves indicate 21 °C and red curves indicate 70 °C. (**A**) Ca-smectite (Ca-sme), (**B**) Na-smectite (Na-sme), (**C**) chlorite (Chl), (**D**) illite (Ill), and (**E**) kaolinite (Kao).

Each sample was mixed with different concentrations of HCl (1, 3, 5, 7, 9, and 12 N) and reacted at 21 and 70 °C. The reaction times were 24 h at 21 °C and 2 h at 70 °C. The samples were then washed with deionized water. The pretreated samples were smeared on glass slides for subsequent analysis. The detailed reaction conditions are presented in Table 1.

Table 1. Reaction conditions.

	Details
Clay Minerals	**Ca-Smectite, Na-Smectite, Chlorite, Illite, and Kaolinite**
Weight	0.05 g
Temperature	21 and 70 °C
Concentration of HCl	1, 3, 5, 7, 9, and 12 N
Time	24 h (21 °C) and 2 h (70 °C)

We also mixed the clay minerals in different proportions and obtained seven mixed-clay samples to assess the effects of HCl on the quantitative analyses. The clay mineral abundances of each mixed sample are listed in Table 2 (the smectite is the mixture of Na-smectite and Ca-smectite as a 1:1 ratio). These seven mixed samples were pretreated with 1, 5, and 12 N HCl at 21 °C and 70 °C, and 1 N acetic acid (HAC) at 21 °C. The samples were then washed with deionized water. The pretreated samples were saturated with a 1 N $MgCl_2$ solution and ethylene glycol, following the routine method [2]. The detailed reaction conditions are listed in Table 2.

Table 2. Clay mineral contents of seven mixed samples (Ill, Chl, Sme, and Kao indicate illite, chlorite, smectite, and kaolinite, respectively).

	Details						
Sample Number	**Std. 1**	**Std. 2**	**Std. 3**	**Std. 4**	**Std. 5**	**Std. 6**	**Std. 7**
Contents (wt.%)	Ill 70, Chl 30	Chl 20, Sme 80	Sme 30, Kao 70	Ill 70, Chl 10, Sme 20	Ill 40, Chl 20, Sme 40	Ill 30, Chl 10, Sme 40, Kao 20	Ill 10, Chl 20, Sme 35, Kao 35
Concentration of HCl	1, 5, and 12 N						
Temperature and reaction time with HCl	21 °C (24 h) and 70 °C (2 h)						
Concentration of HAC	1 N						
Temperature and reaction time with HAC	21 °C (24 h)						

Major and minor elements in each mineral (Ca-smectite, Na-smectite, chlorite, illite, and kaolinite) were analysed before and after pretreatment with 12 N HCl at 70 °C. Due to the limited remaining clay material after HCl pretreatment, analysis by X-ray fluorescence spectrometry (XRF) was not possible. As such, an inductively coupled plasma optical emission spectrometer (ICP–OES) (Thermo Fisher) was used to test the element composition of these samples at the Rock–Mineral Preparation and Analysis Laboratory, Institute of Geology and Geophysics, Chinese Academy of Sciences. Prior to ICP–OES analysis, the samples (6 mg) were dissolved in a mixture of HNO_3, HF, and $HClO_4$ in a Teflon capsule at 140 °C on a hotplate for 5 h. The digested samples were diluted with 1% HCl for ICP–OES analysis. The precision of the elemental analyses was better than ± 5%.

We also examined the clay mineral structure after pretreatment with 12 N HCl at 70 °C by transmission electron microscopy (TEM) and energy dispersive spectroscopy (EDS), using a JEOL JEM-2100 instrument at the Electron Microscopy Laboratory, Institute of Geology and Geophysics, Chinese Academy of Sciences.

2.2. Comparison between the HCl Pretreatment and Routine Methods

We mixed the five clay mineral samples in different proportions and obtained 24 mixed samples for analysis by the HCl pretreatment and routine methods (the smectite is the mixture of Na-smectite and Ca-smectite as 1:1 ratio). The mineral abundances of each sample are listed in Table S3. These 24 mixed samples were pretreated with 1 N HCl at 70 °C and then washed with deionized water. The pretreated samples were saturated with a 1 N $MgCl_2$ solution and ethylene glycol, following the routine method for quantitative analysis of clay minerals.

We also selected 19 Pliocene red clay samples from the southern Chinese Loess Plateau to assess the differences in the paleoclimatic conditions obtained from the clay mineral index by the HCl pretreatment and routine methods [24].

The HCl pretreatment method employed the bulk sample XRD measurements and intensity of the main XRD reflection peak to determine the relative contents of each mineral [9]. The bulk samples were ground to <45 μm in an agate mortar and compacted into a random orientation on glass slides. The XRD patterns were obtained with Ni-filtered Cu-Ka radiation at a voltage of 40 kV and beam intensity of 40 mA. The scan range was 2θ = 2–70°. After the XRD measurements, the samples were heated at 70 °C in 1 N HCl for 3 h to remove chlorite and then repeatedly washed with deionized water. The same XRD measurements were then repeated. Mineral identification was based on the intensity of the following peaks: smectite = 14.33 Å, illite = 10.00 Å, chlorite and kaolinite = 7.10 Å, quartz = 3.33 Å, albite = 3.18 Å, and calcite = 3.02 Å. The peak at ~12.5° in the XRD patterns of the HCl-treated samples was regarded to reflect kaolinite, and the decrease of this peak height reflected the chlorite content. The peak height for each mineral was determined using Highscore software.

The routine method first involved the extraction of the clay fraction (<2 μm) and saturation with 1 N $MgCl_2$. The $MgCl_2$ replaces the cations within the interlayers of the clay minerals and reduces the d-spacing variability [8]. To identify the expanding clay minerals, ethylene glycol was added to the Mg^{2+}-saturated samples. The samples were then centrifuged to concentrate the clay minerals into a paste that was spread onto calibrated recesses on glass slides to obtain oriented samples. XRD analysis was conducted with a step size of 0.020° and scan rate of 0.050° s^{-1} at 2θ = 3–30°. To determine the relative contents of chlorite and kaolinite, slow scanning was undertaken at 2θ = 24–26°. Quantitative analysis was carried out following the routine method on the areas of the main basal reflections, which are the (001) peak of smectite (17 Å), (001) peak of illite (10 Å), (002) peak of chlorite, and (001) peak of kaolinite (7.1 Å). The contents of each clay mineral (illite, chlorite, kaolinite, smectite) were determined follow the 100% normalized mineral intensity factor method [25–27]. The weighting factors were: 4 for illite, 2 for chlorite, and 1 for smectite [26,28]. Although, some other weighting factors were also introduced [29,30], the one we chose were widely used in the clay mineral paleoclimate reconstruction [2,6,15,31,32]. The ratio of chlorite to kaolinite was determined by the area ratio of the (004) peak of chlorite (3.54 Å) with respect to the (002) peak of kaolinite (3.58 Å) [26]. The quantification analysis was calculated by MacDiff software (MacDiff 4.2.5, Rainer Petschick, Frankfurt, Germany) [33]. The analytical precision obtained from replicates ranged from ±1.44% to ±3.09% (2σ) for each clay mineral and had an accuracy of ~5% [31]. All the clay mineral data were generated under exactly the same analytical method using the same X-ray diffractometer (PANalytical) with Ni-filtered Cu-Kα radiation (40 kV and 40 mA) at the Laboratory of Soil Geology and Environment, Institute of Geology and Geophysics, Chinese Academy of Sciences.

3. Results

3.1. Individual Clay Mineral Samples with Different HCl Pretreatments

The crystal structures of the individual clay mineral samples differed with the pretreatment. The XRD patterns for each mineral with different pretreatment conditions are shown in Figure 1.

We used the intensity and full width at half maximum (FWHM) of the main XRD reflection peaks for each clay mineral to evaluate the crystal structures after different HCl pretreatments. In detail, we used the ratios of these parameters for each pretreatment condition to those without HCl pretreatment (Figure 2).

To assess the leaching from the different clay minerals caused by the HCl, we determined the major and minor element concentrations before and after pretreatment with 12 N HCl at 70 °C (Table 3). Before HCl pretreatment, the ICP–OES and XRF methods yielded identical elemental concentrations for the five clay mineral samples (Table S2). Given that the SiO_4 groups in the tetrahedral sheet of the clay minerals were intact after HCl pretreatment, the lack of Si data obtained from the ICP–OES analysis did not affect our observations.

Table 3. Major and minor element concentrations (μg/g) in samples pretreated with 12 N HCl at 70 °C as compared with the original samples.

Elements	Al	Ca	Fe	K	Mg	Na	Ti	Zn	Ba	Sr
HCl–Ca-Sme	17.26	2.07	3.09	1.15	3.80	2.52	0.20	0.17	0.06	0.06
Ca-Sme	49.2	11.8	8.43	2.40	17.2	2.86	0.50	0.20	0.30	0.14
HCl–Na-Sme	47.3	2.14	5.44	2.67	9.66	3.93	0.40	0.18	0.06	0.08
Na-Sme	60.4	9.66	7.23	3.26	13.4	20.9	0.46	0.21	0.17	0.23
HCl–Chl	1.96	2.02	2.85	0.40	81.4	2.70	1.24	0.15	0.04	0.07
Chl	24.6	4.43	7.16	0.41	109	2.50	0.67	0.16	0.05	0.10
HCl–Ill	59.4	2.62	2.95	15.7	2.00	3.82	3.47	0.18	0.32	0.15
Ill	75.7	2.48	3.76	18.7	2.44	3.84	3.70	0.16	0.36	0.20
HCl–Kao	135	2.24	2.82	2.22	0.42	2.61	1.52	0.18	0.07	0.09
Kao	122	3.01	4.84	1.98	0.43	3.68	1.32	0.25	0.08	0.11

The two types of smectite exhibited different behaviours during the HCl pretreatment. HCl concentrations of >3 N at 70 °C or >7 N at 21 °C can dissolve most Ca-smectite (Figures 1A and 2A). The much higher FWHM ratio of the Ca-smectite pretreated with HCl indicates there was considerable damage to the Ca-smectite structure (Figure 2A). All the major elements, except Na, are mostly leached out by the 12 N HCl at 70 °C (Table 3). The TEM images show that the specific surface area increased after HCl pretreatment, which indicated that the original platy crystal shape was fractured and the dissolved crystal rims were warped (Figure 3A,B).

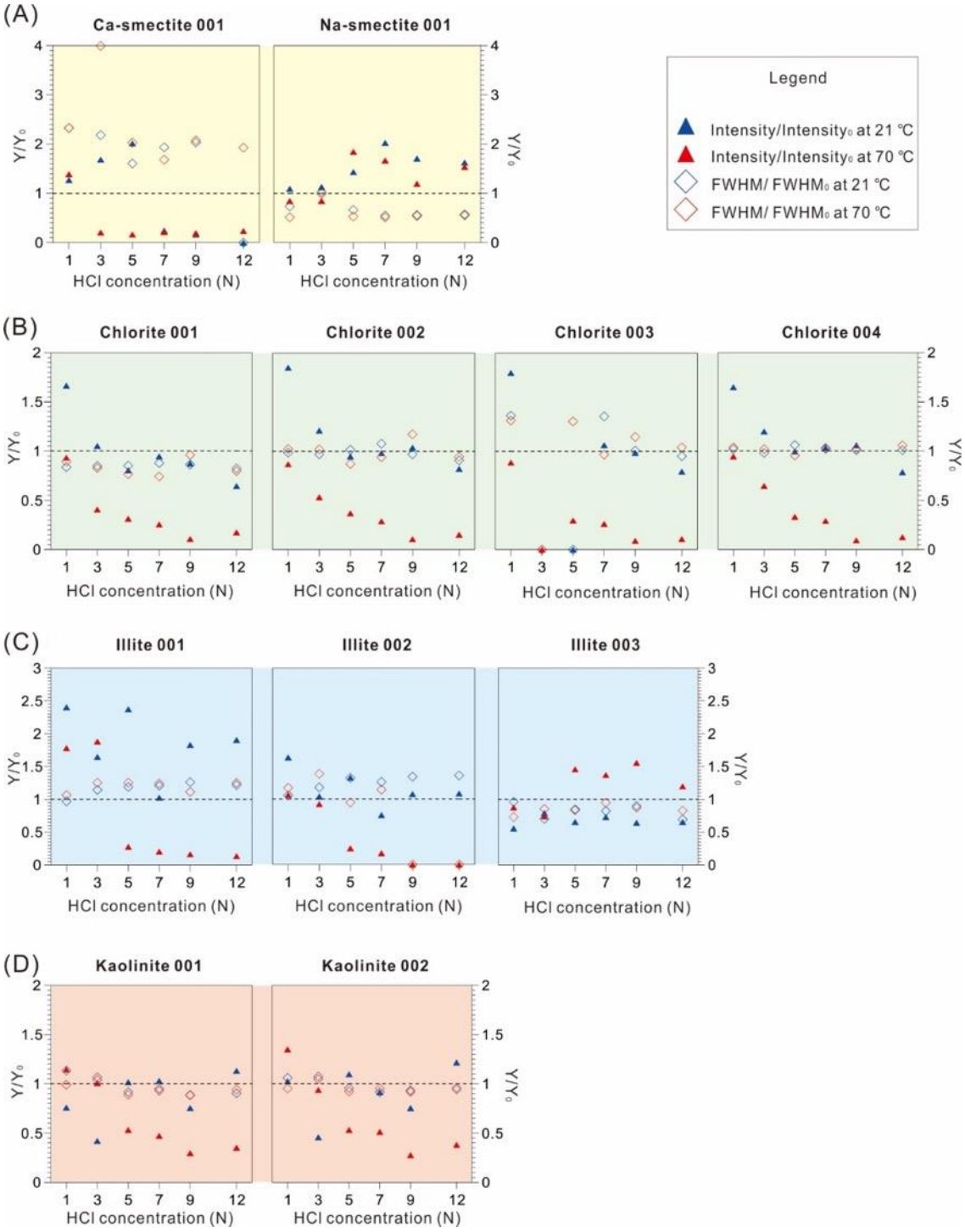

Figure 2. Ratios of the XRD pattern parameters (i.e., intensity and full width at half maximum (FWHM)) after different pretreatments for Ca-smectite, Na-smectite, chlorite, illite, and kaolinite for each reflection. The y-axis (Y/Y_0) is the ratio of the reflection after pretreatment to that with no pretreatment, which is intensity/intensity$_0$ and FWHM/FWHM$_0$. The x-axis is the concentration of HCl. (**A**) Ca-smectite and Na-smectite, (**B**) chlorite, (**C**) illite, and (**D**) kaolinite.

For Na-smectite, all HCl concentrations barely dissolved the mineral at either reaction temperature (Figure 1B). However, the HCl pretreatment changed the shape of the (001) peak from relatively broad to sharp with an asymmetric ridge. The HCl pretreatment also changed the position of the (001) peak to a lower 2θ angle, with a range even greater than that of Ca-smectite. The FWHM ratio of the Na-smectite shows that the peak became narrower after HCl pretreatment (Figure 2A). After pretreatment with 12 N HCl at 70 °C,

the concentrations of all major elements decreased. The variations in most major elements (i.e., except Na) were smaller than those of Ca-smectite. The TEM images indicated that HCl pretreatment had little effect on the main crystal structure of Na-smectite (Figure 3C–D).

Chlorite exhibited the largest changes as a result of HCl pretreatment. As the HCl concentration and reaction temperature increase, the intensity ratios of the (001), (002), (003), and (004) peaks of chlorite decrease (Figure 2B). Pretreatment of 9 N HCl at 70 °C had the strongest dissolution effect and dissolves most of the chlorite (Figure 1C). The (001) and (002) peaks of residual chlorite after HCl pretreatment were not broadened (Figure 2B). The main cations in chlorite are Si, Al, Fe, and Mg (Table S1) [23]. After pretreatment with 12 N HCl at 70 °C, the chlorite concentrations of Al and Fe had decreased by >60%, and those of Ca and Mg decreased significantly but not by more than 50% (Table 3). The TEM–EDS data for chlorite showed that after pretreatment with 12 N HCl at 70 °C, the Si and Al concentrations in chlorite decreased significantly, which indicated the crystal structure was destroyed (Figure 3E–F).

The dissolution of illite increased at higher temperatures (70 °C). Pretreatment of 5 N HCl at 70 °C was the threshold for illite dissolution (Figure 1D). Above this HCl concentration at 70 °C, the intensities of the (001), (002), and (003) peaks declined abruptly. The FWHM indicates that illite was little affected at lower temperatures, and that 7 N HCl at 70 °C can significantly damage illite (Figure 2C). After pretreatment with HCl (especially at 21 °C), a broad peak appeared at ~7.5 Å (Figure 1D). After heating to 350 °C, the broad peak at ~7.5 Å became narrower and shifted to 7.1 Å (Figure S1). This indicated the presence of halloysite in the illite sample, and that its content increased slightly during pretreatment at low HCl concentrations. The decreasing Al, Fe, and K concentrations also indicate that crystal damage occurred to illite at high HCl concentrations at 70 °C (Table 3). The TEM images suggested that the larger plates of illite with straight and sharp edges became fractured and developed rounded edges. Rod-like kaolinite-group minerals appeared after HCl pretreatment (Figure 3I–J). Cations such as Na^{+}, Mg^{2+}, and K^{+} were leached out during HCl pretreatment.

For kaolinite, the intensity ratios indicated that at the lower temperature (21 °C), lower HCl concentrations (1 and 3 N) probably had a stronger dissolution effect. At the higher temperature (70 °C), dissolution increased with increasing HCl concentrations. However, compared with the other clay minerals, kaolinite dissolution in HCl was limited. The FWHM ratios of the peaks exhibited little variation (Figure 2D). The major and minor element concentrations were largely invariant, even at the highest HCl concentration (Table 3). The TEM images of kaolinite suggested that the HCl had little effect on its crystal surface, shape, or structure (Figure 3K–L).

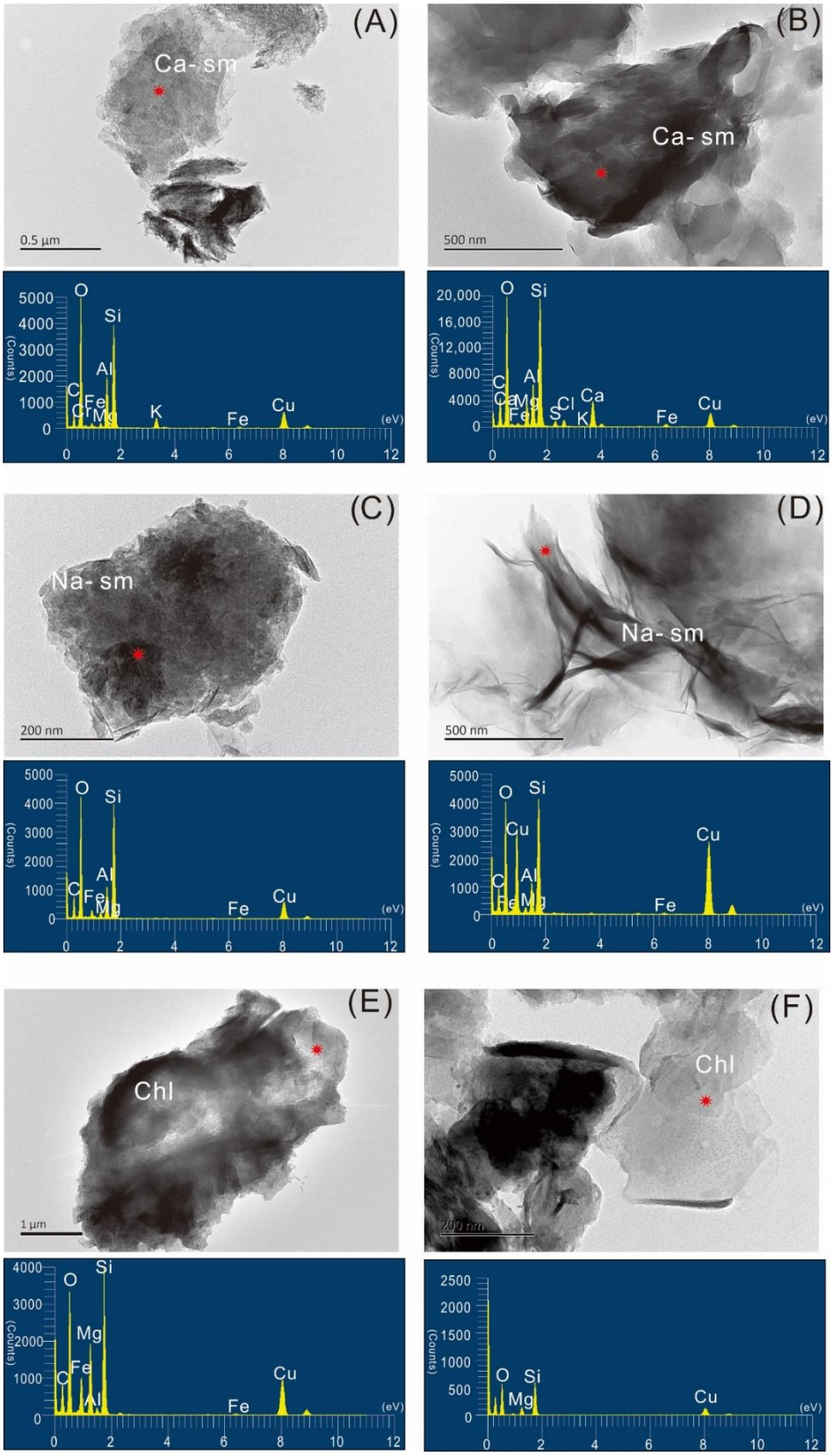
(A)
Ca- sm
0.5 µm
(B)
Ca- sm
500 nm
(C)
Na- sm
200 nm
(D)
Na- sm
500 nm
(E)
Chl
1 µm
(F)
Chl
200 nm
(Counts)
(eV)
O
Si
Al
C
Fe
Mg
K
Cu
Ca
Cl
S

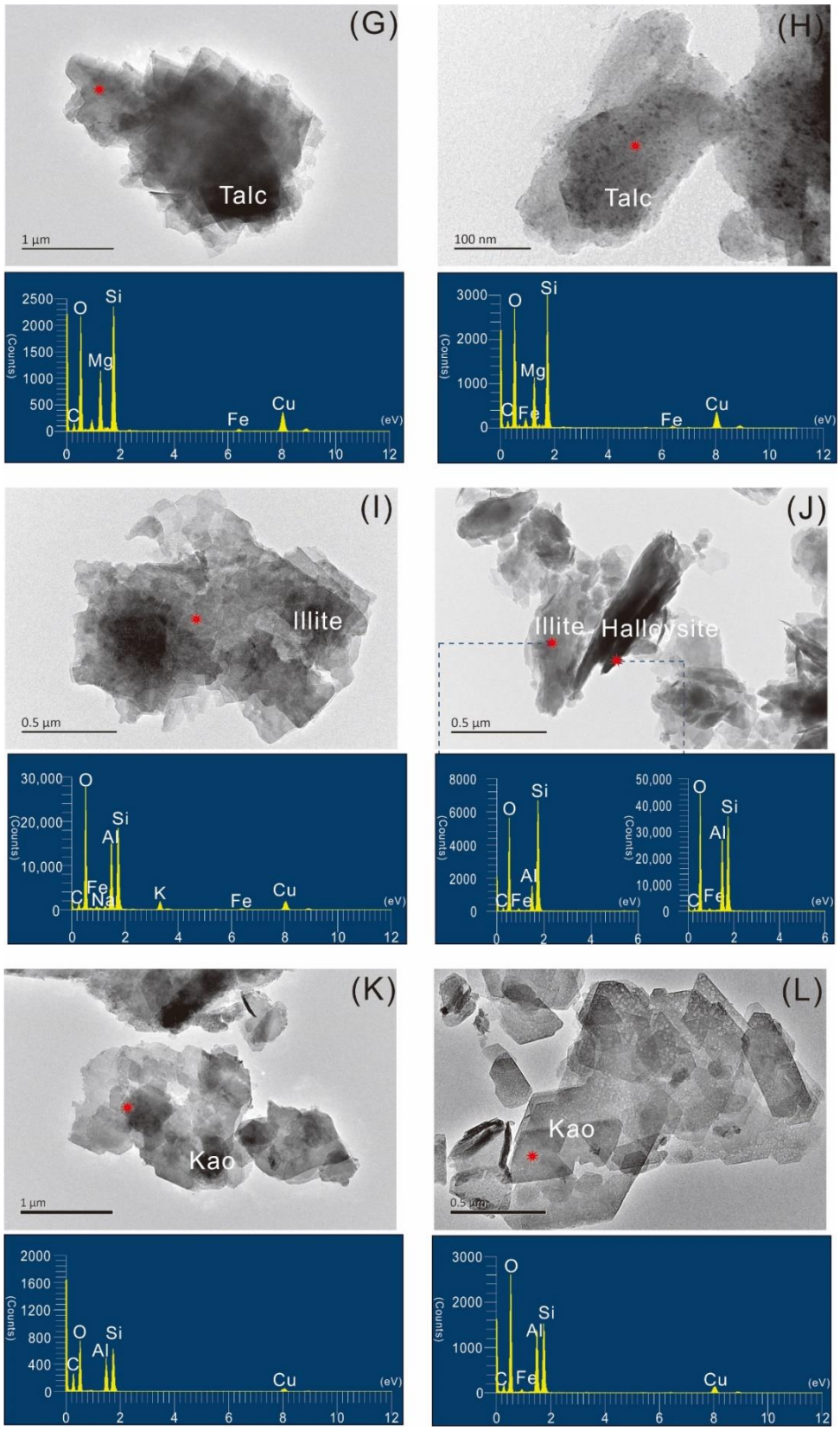

Figure 3. TEM images of the clay minerals (**A**, **C**, **E**, **G**, **I**, and **K**) without pretreatment and (**B**, **D**, **F**, **H**, **J**, and **L**) after pretreatment with 12 N HCl at 70 °C. Ca-smectite (Ca-Sm) (**A**) before and (**B**) after HCl pretreatment; Na-smectite (Na-Sm) (**C**) before and (**D**) after HCl pretreatment; chlorite (Chl) (**E**) before and (**F**) after HCl pretreatment; talc (**G**) before and (**H**) after HCl pretreatment; illite (**I**) before and (**J**) after HCl pretreatment; kaolinite (Kao) (**K**) before and (**L**) after HCl pretreatment. The red stars mark the sites where EDS data were obtained.

3.2. Mixed Samples Subjected to Different HCl Pretreatments

The effects of different pretreatment conditions on the quantification of clay minerals were shown in Figure 4. The variation in the data obtained for the mixed samples that contained two minerals (Std. 1, 2, and 3) was smaller than that for samples that contained three or four minerals. For the mixed samples with two minerals, the contents of each mineral after different pretreatments did not vary by >20%. However, for the mixed samples with three minerals (Std. 4 and 5), the low-solubility minerals (illite and smectite) exhibited highly variable contents (28%–72% and 15%–67%, respectively). In general, as the HCl concentration increased, the variations in mineral content increased. Interestingly, for Std. 4 and 5, as the HCl concentration increased, the relative content of chlorite increased. This might be explained by the formation of a kaolinite-like mineral at 7 Å. For the mixed samples with four minerals, where both chlorite and kaolinite were present, a high HCl concentration at 70 °C removed chlorite but not kaolinite. The analyses of the mixed samples with four minerals were also variable after different pretreatments. For Std. 6 and 7, the relative contents of smectite varied from 21% to 67% and those of kaolinite from 20% to 61%. The increasing kaolinite content at high HCl concentrations can be attributed to the increase in the 7 Å peak due to leaching of illite and Ca-smectite.

The pretreatment at 1 N HCl had the least effects (Figure 4), and 1 N HCl can more easily dissolve chlorite at 70 °C than 21 °C. Based on the different effects of the HCl pretreatment conditions on the individual and mixed clay samples, we used 1 N HCl at 70 °C to dissolve chlorite and avoid the dissolution of other clay minerals when undertaking a comparison of the HCl pretreatment and routine methods.

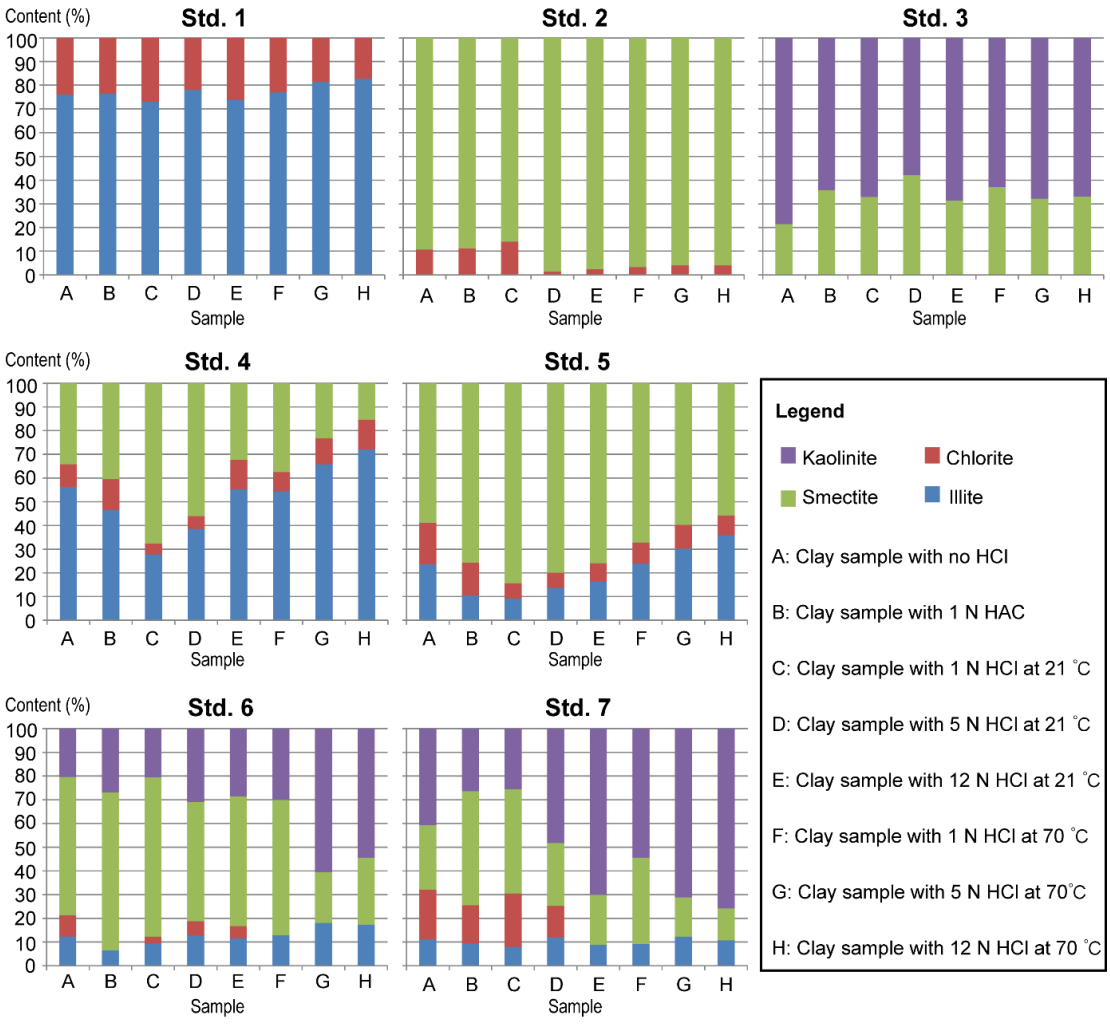

Figure 4. Quantification of the mixed clay samples after different pretreatments.

3.3. Comparison of the HCl Pretreatment and Routine Methods in Analysing Mixed and Natural Samples

To compare the HCl pretreatment and routine methods, we mixed the five clay minerals in different proportions to make 24 mixed samples (Table S3). The results of clay mineral analysis obtained with the HCl pretreatment and routine methods are shown in Figure 5. We examined the correlation between the height of the main XRD reflection after HCl pretreatment and the actual mass content of each clay mineral. We also examined the correlation between the mineral abundances obtained from the routine method and the actual mass content of each clay mineral (Figure 5). The R^2 values of these linear correlations reflect the accuracy of the clay mineral determinations by the two methods. The R^2 value from the data obtained after HCl pretreatment is lower than that of the routine method, particularly for chlorite and smectite. This suggests that the accuracy of the HCl pretreatment method is lower than that of the routine method.

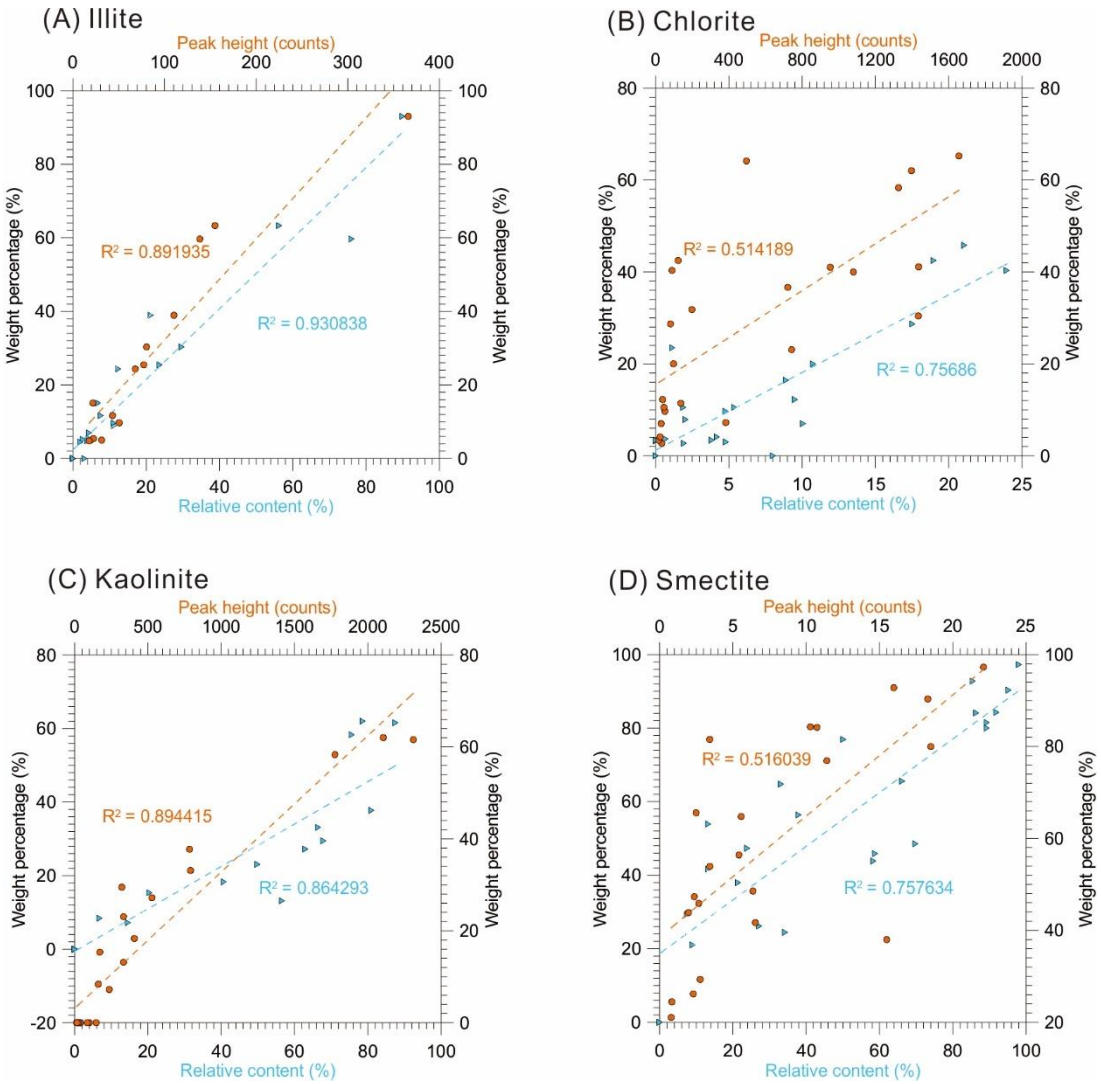

Figure 5. Results of clay mineral analysis obtained with the two methods and the actual clay contents of the 24 mixed standard samples. The orange dashed lines are the linear correlations between the height of the main XRD reflection after HCl pretreatment and the actual clay contents. The blue dashed lines are the linear correlations between the results obtained from the routine method and the actual clay contents. (**A**) Illite, (**B**) chlorite and kaolinite, (**C**) kaolinite, and (**D**) smectite.

Figure 6 shows the results of the clay mineral analyses of 19 natural samples with the HCl pretreatment and routine methods. The XRD patterns from the two methods

show that the clay minerals present are illite, chlorite, kaolinite, and smectite (Figure 6A). The bulk samples also contain detrital quartz and albite.

Figure 6B–F show the variations in the contents of each clay mineral and paleoclimate proxy with depth for the 19 red clay samples. We also compared a paleoclimate proxy, the smectite/(illite + chlorite + kaolinite) ratio that distinguishes between dry and wet climate (Figure 6F). The kaolinite contents obtained from the two methods exhibit greater differences than those obtained for the other minerals (Figure 6B–E). The two methods yielded similar variability in the smectite/(illite + chlorite + kaolinite) ratios, although the ratios obtained by the HCl pretreatment method were higher than those obtained from the routine method.

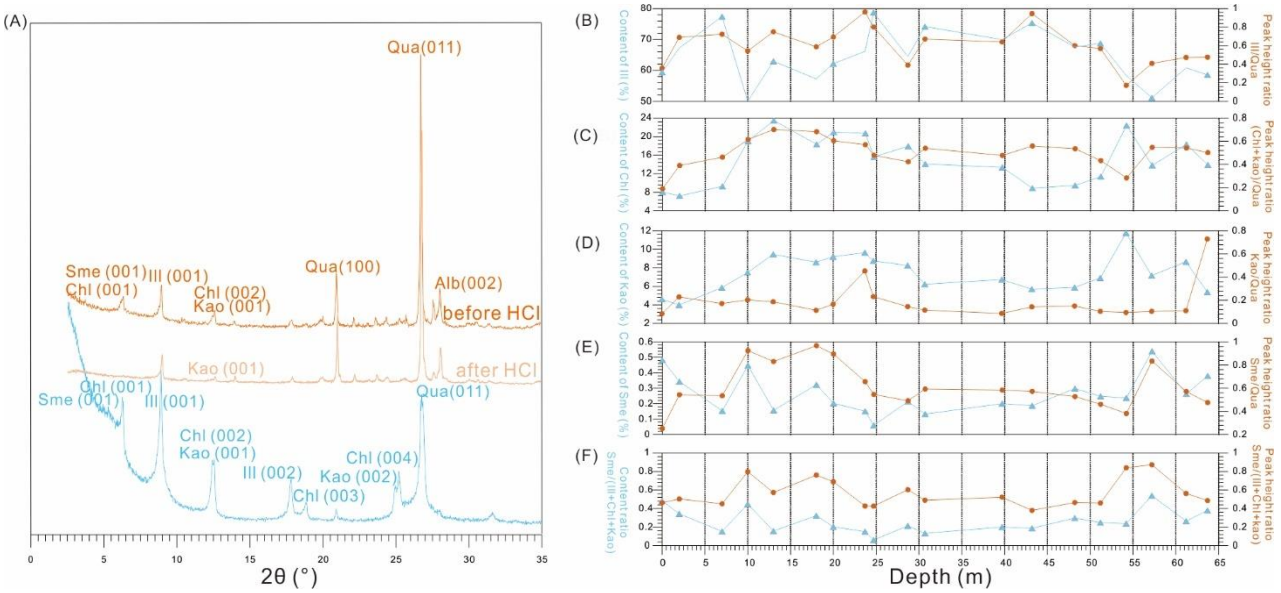

Figure 6. Comparison of the XRD patterns and data obtained for the natural red clay samples versus depth using the HCl pretreatment and routine methods. The orange curves are the ratios of the main XRD reflection height with pretreatment of 1 N HCl at 70 °C (smectite at 14.33 Å, illite at 10.00 Å, chlorite and kaolinite at 7.10 Å before HCl pretreatment; kaolinite at 7.10 Å after HCl pretreatment) to the height of the quartz peak at 3.33 Å. The blue curves are the relative contents of each clay mineral obtained with the routine method. (**A**) XRD pattern of a representative natural red clay sample. Sme = smectite, Chl = chlorite, Ill = illite, Kao = kaolinite, Qua = quartz, and Alb = albite. (**B**) Depth changes of the main XRD peak height ratio of Ill (001)/Qua (011) and relative content of Ill. (**C**) Depth change of the main XRD peak height ratio of Chl (002) + Kao (001)/Qua (011) and relative content of Chl. (**D**) Depth change of the main XRD peak height ratio of Kao (001)/Qua (011) and relative content of Kao. (**E**) Depth change of the main XRD peak height ratio of Sme (001)/Qua (011) and relative content of Sme. (**F**) Depth change of the paleoclimate proxy Sme (001)/(Ill (001) + Chl (002) + Kao (001) and Sme/(Ill + Chl + Kao) ratio.

4. Discussion

4.1. Effects of HCl Pretreatment on the Structure of Individual Clay Minerals

The effects of HCl pretreatment depend on the mineral structure of the various clays. All the clays comprise two structural units: tetrahedral and octahedral sheets [8]. The octahedral sheets can be classified as dioctahedral or trioctahedral based on the cation/anion ratio. Clay minerals in HCl lose exchangeable cations and Al, Mg, and Fe from the octahedral and tetrahedral sheets, but the SiO_4 groups in the tetrahedral sheets remain largely intact [34]. As such, the main effect of HCl on the clay mineral structure is corrosion of the octahedral sheets, although previous experimental studies have shown that the dissolution rate of Al^{3+} is the same in the tetrahedral and octahedral sheets [35]. The dissolution rates of the two kinds of octahedral sheet are different: the dissolution rate of trioctahedral layers is much higher than that of dioctahedral layers [36,37]. The greater substitution of

Mg^{2+} and/or Fe^{3+} for Al^{3+} in dioctahedral smectites increases their dissolution rate in HCl [38].

Chlorite is a 2:1 layer clay (i.e., two tetrahedral sheets and one octahedral sheet) with an interlayer sheet of octahedrally coordinated cations by hydroxyls. Most chlorite in sedimentary rocks is trioctahedral and varies from Mg- to Fe-rich chlorite [8]. Given that the trioctahedral species are more soluble in HCl, all HCl concentrations used in our experiments could dissolve chlorite, and an increase in temperature also enhanced dissolution. The studied chlorite was Mg-rich and was less affected by HCl than Fe-rich chlorite [8]. 1 N HCl was sufficient to dissolve most of the chlorite in the natural samples.

Kaolinite is a 1:1 layer clay. The structural unit of kaolinite is formed by the superposition of a tetrahedral sheet on a dioctahedral sheet. HCl cannot effectively dissolve kaolinite without calcination, and the dissolution effect is much less than that of H_2SO_4 and alkali [22]. In the present study, lower HCl concentrations and high temperatures did not affect the kaolinite mineral structure.

Illite is a 2:1 dioctahedral phyllosilicate. K^+ is the interlayer cation in a unit comprising two tetrahedral sheets and one dioctahedral sheet. The crystal structure of illite is similar to that of smectite, but it is non-swelling and has a lower cation exchange capacity [39]. In the present study, illite was more resistant to HCl dissolution, similar to kaolinite and consistent with a previous study [40]. This may be because kaolinite and illite have more dioctahedral sheets in their crystal structures, which are more resistant to HCl dissolution. However, the increase of the broad 7.5 Å peak indicates the dissolution of illite. The tubular morphology in the TEM images, and movement of the XRD reflection peak to 7.1 Å at 350 °C, indicate the presence of dehydrated halloysite. Even so, as the halloysite content is low, the mechanism of illite dissolution in HCl is likely to be the same as that described in previous studies. The dissolution probably initiated along the OH groups at the edges of the octahedral sheets, and the release of K^+ was slower than the leaching of the octahedral cations [38]. This is consistent with the larger decrease in Al as compared with K after HCl pretreatment (Table 3).

Smectite is a hydrated 2:1 layered dioctahedral aluminosilicate that is characterized by swelling and a high cation exchange capacity. Smectite comprises two tetrahedral sheets that are bonded to either side of an octahedral sheet, similar to illite. The isomorphous substitution of Mg^{2+} for octahedral Al and Al^{3+} for tetrahedral Si results in a charge deficit. This layer charge is balanced by hydrated exchangeable cations that occupy the surfaces between the clay layers, termed the interlayer [20]. The two types of studied smectites exhibited different HCl dissolution behaviours that can be attributed to the different substitutions of the octahedral cations. Aluminium contents are higher in Na-smectite than Ca-smectite, whereas Mg–Fe contents exhibit the opposite trend (Table S1). This indicates that there is more Mg^{2+} and Fe^{3+} substitution for octahedral Al in the Ca-smectite. The two types of smectite exhibited large decreases in interlayer cation contents after HCl pretreatment; i.e., for Ca in Ca-smectite and Na in Na-smectite (Table 3). The large decreases in Al and Mg contents suggest that damage of the dioctahedral sheet is more severe in Ca-smectite than in Na-smectite. Therefore, smectite dissolution in HCl involves the leaching of interlayer cations by protons, followed by the removal of the central atoms in the octahedral sheets. The octahedral sheets in smectite with more Mg^{2+} are more readily dissolved by HCl because the electrostatic bond between Al–O ions is stronger than for Mg–O ions [41]. This dissolution mechanism is consistent with that proposed in a previous study [34].

4.2. Effects of HCl Pretreatment on the Identification and Quantification of Clay Minerals in Mixed Samples

Based on the effects of HCl pretreatment on the individual clay minerals, chlorite can be distinguished from kaolinite, and the different structures of smectite can be identified

in the mixed samples by using HCl pretreatment. Specifically, 1 N HCl at 70 °C can dissolve most chlorite, but little kaolinite and other clay minerals, whereas 3 N HCl at 70 °C can distinguish between the smectites with different structures.

The analyses of the mixed samples are affected by the dissolution of minerals and the formation of new phases in the HCl. At >3 N HCl, the dissolved minerals are chlorite and Ca-smectite, and illite is partly dissolved, leading to an XRD peak at 11–12° (7.0–7.5 Å) that overlaps with the kaolinite peak. Therefore, HCl pretreatment of clay minerals should employ an acid strength of ≤1 N.

The analysis of the mixed samples after pretreatment with 1 N HCl at 70 °C shows that apart from kaolinite, the accuracy of the HCl pretreatment method is lower than that of the routine method (Figure 5). This is because in the bulk sample XRD analysis used in the HCl pretreatment method, the non-clay minerals tend to disrupt the preferred orientation of the clay minerals [8,42]. Nevertheless, the analyses with the routine method also exhibit deviations from the actual mass contents of each clay mineral in the mixed samples. This is because the contents obtained with the routine method are the volume percentage of each clay mineral.

4.3. Estimation of the Clay Mineral Index in Natural Samples with the HCl Pretreatment Method

Paleoclimate reconstructions using the clay mineral index require thousands of analyses, and the routine method is time-consuming. Some studies of sediment samples with high contents of clay minerals and known mineral species have simplified this procedure by using bulk samples and the HCl pretreatment method [9]. We compared results obtained after pretreatment with 1 N HCl at 70 °C and those obtained with the routine method.

The two methods yield different contents of clay minerals (Figure 6B–E). The largest differences are for kaolinite and chlorite (Figure 6C–D). This can be attributed to the lower accuracy of the HCl pretreatment method. However, the variations of the clay mineral index obtained with the two methods are similar (Figure 6F).

Previous studies have suggested that smectite forms mostly after moderate chemical weathering, which is indicative of a warm and humid climate, whereas illite and chlorite are the products of physical weathering and are indicative of a cool and dry climate [43–45]. The paleoclimate of temperate regions (including the Chinese Loess Plateau) does not favour the production of authigenic kaolinite, and the small amount of kaolinite in our samples is probably detrital [15]. The ratio of smectite to the sum of detrital minerals is an index of the weathering intensity. Because the kaolinite contents are low (<10%) in the present results, the two methods yield similar variations in the clay mineral index. However, with respect to the weathering intensity, the ratio obtained using the HCl pretreatment method is obviously higher than that obtained using the routine method (Figure 6F). This suggests that the HCl pretreatment method yields results that erroneously indicate humid conditions.

In summary, compared with the routine method, bulk XRD analysis after HCl pretreatment is less accurate, and the latter method is not suitable for determination of the clay mineral index.

4.4. Effect of HCl Pretreatment in Other Experiments

HCl pretreatment is used to remove carbonate cement prior to the grain size analysis of sedimentary rocks and clay mineral separation. The common pretreatment procedure involves dissolution in 10% HCl (~3.33 N) under boiling conditions [16]. However, given the dissolution of illite, chlorite, and smectite documented in our study, this pretreatment is probably dissolving the fine-grained fraction. We suggest that such pretreatment for grain size analysis should use <1 N HCl.

Moreover, our results can guide other chemical pretreatment procedures used in mineral separation, such as the O isotope analysis of specific minerals [17,18,46]. In such

studies, 10% HCl is used to remove chlorite or 1 N HCl, 5 N NaOH, and 6 N HCl are used sequentially to obtain relatively pure hematite. However, based on our data, 10% HCl can dissolve not only chlorite but also Ca-smectite, and boiling 6 N HCl can remove hematite and residual illite from the previous 1 N HCl and 5 N NaOH pretreatment.

5. Conclusions

We examined the crystal structures of illite, chlorite, kaolinite, and two types of smectite after pretreatment with different concentrations of HCl at various temperatures. We compared the results with those obtained by the routine method for mixed standard and natural clay samples. Our results can guide the use of acid pretreatment of clays prior to determination of paleoclimate proxy data and quantification of clay mineral abundances. Our main conclusions are as follows.

1. Chlorite is the most soluble clay mineral in HCl and can be effectively dissolved in HCl with a concentration of >1 N. The different crystal structures of smectite exhibit differences in HCl dissolution. Ca-smectite with more substituted octahedral Al can be dissolved with HCl. Na-smectite is barely dissolved at any HCl concentration or temperature. Illite is partly dissolved in HCl, at ≥5 N HCl at 70 °C. Kaolinite is not effectively dissolved in HCl.
2. The XRD peak of residual illite at 11–12° (7.0–7.5 Å) after HCl pretreatment is the main source of error in the identification and quantification of clay minerals by this method. 1 N HCl at 70 °C can dissolve most chlorite with limited effects on the other clay minerals. 3 N HCl at 70 °C can distinguish between the different types of smectite.
3. The quantification of clay mineral contents from the peak heights of bulk sample XRD data after HCl pretreatment is less accurate than the routine method. Therefore, it is not suitable for the analysis of clay minerals for paleoclimate studies.
4. The effects of HCl pretreatment on clay minerals in other types of research (e.g., grain size analysis and chemical pretreatment of mineral separates) needs to be considered. Ideally, the HCl concentration should be <1 N to avoid digestion of clay minerals.

Supplementary Materials: The following supporting information can be downloaded at https://www.mdpi.com/article/10.3390/min12091167/s1: Table S1: Major and minor element concentrations of kaolinite, Na-smectite, Ca-smectite, chlorite, and illite samples used in this study, as measured by XRF; Table S2: Comparison of the relative element contents obtained by ICP–OES and XRF; Table S3: Clay mineral contents of 24 mixed standard samples (Ill, Chl, Sme, and Kao indicate illite, chlorite, smectite, and kaolinite); Figure S1: XRD reflection of illite after 3N HCl pretreatment at 21 °C. The black line is for the analysis at room temperature, and the red line is for the analysis at 350 °C. The blue data are for the slow speed scan at 2θ = 10–21°.

Author Contributions: Conceptualization, C.Z.; software, B.H.; validation, B.H.; formal analysis, B.H.; resources, X.Z.; writing—review and editing, C.Z. and B.H. All authors have read and agreed to the published version of the manuscript.

Funding: This research was supported by the National Natural Science Foundation of China (grants 42072209, 41722206, 41690114, 41888101, and 42107473), the Strategic Priority Research Program of the Chinese Academy of Sciences (grant XDB26000000), and the International Cooperation Program of the Chinese Academy of Sciences (grant 131C11KYSB20160061).

Data Availability Statement: The data used to support the findings of this study are available from the first author upon request.

Acknowledgments: We thank Tang Xu from the Electron Microscopy Laboratory, Institute of Geology and Geophysics, Chinese Academy of Sciences, for help with the TEM analyses and Yifan Lv for providing samples of red clay.

Conflicts of Interest: The authors declare no conflicts of interest.

References

1. Ehlmann, B.L.; Mustard, J.F.; Murchie, S.L.; Bibring, J.P.; Meunier, A.; Fraeman, A.A.; Langevin, Y. Subsurface Water and Clay Mineral Formation During The Early History of Mars. *Nature* **2011**, *479*, 53–60. https://doi.org/10.1038/nature10582.
2. Zhang, C.; Guo, Z. Clay Mineral Changes Across The Eocene–Oligocene Transition in The Sedimentary Sequence at Xining Occurred Prior to Global Cooling. *Palaeogeogr. Palaeoclimatol. Palaeoecol.* **2014**, *411*, 18–29. https://doi.org/10.1016/j.palaeo.2014.06.031.
3. Pearson, V.K.; Sephton, M.; Kearsley, A.T.; Bland, P.A.; Franchi, L.A.; Gilmour, l. Clay Mineral-Organic Matter Relationships in The Early Solar System. *Meteorit. Planet. Sci.* **2002**, *37*, 1829–1833. https://doi.org/10.1111/j.1945-5100.2002.tb01166.x.
4. Yaremchuk, Y.; Hryniv, S.; Peryt, T.; Vovnyuk, S.; Meng, F. Controls on Associations of Clay Minerals in Phanerozoic Evaporite Formations: An Overview. *Minerals* **2020**, *10*, 974. https://doi.org/10.3390/min10110974.
5. Zhang, M.; Lu, H.; Chen, Q.; Bandara, G.; Zhang, H.; Luo, C.; Wu, N. Clay Mineralogy and Geochemistry of the Pockmarked Surface Sediments from the Southwestern Xisha Uplift, South China Sea: Implications for Weathering and Provenance. *Geosciences* **2020**, *11*, 8. https://doi.org/10.3390/geosciences11010008.
6. Hu, B.; Zhang, C.; Wu, H.; Hao, Q.; Guo, Z. Clay Mineralogy of An Eocene Fluvial-Lacustrine Sequence in Xining Basin, Northwest China, and Its Paleoclimatic Implications. *Sci. China Earth Sci.* **2019**, *62*, 571–584. https://doi.org/10.1007/s11430-018-9282-8.
7. Piga, G.; Santos-Cubedo, A.; Brunetti, A.; Piccinini, M.; Malgosa, A.; Napolitano, E.; Enzo, S. A Multi-Technique Approach by XRD, XRF, FT-IR to Characterize The Diagenesis of Dinosaur Bones From Spain. *Palaeogeogr. Palaeoclimatol. Palaeoecol.* **2011**, *310*, 92–107. https://doi.org/10.1016/j.palaeo.2011.05.018.
8. Moore, D.M.; Reynolds, R.C. X-ray Diffraction and the Identification and Analysis of Clay Minerals; Oxford University Press: Berlin, Germany, 1997.
9. Sun, Y.; Ma, L.; Bloemendal, J.; Clemens, S.; Qiang, X.; An, Z. Miocene Climate Change on The Chinese Loess Plateau: Possible Links to The Growth of The Northern Tibetan Plateau and Global Cooling. *Geochem. Geophys. Geosystems* **2015**, *16*, 2097–2108. https://doi.org/10.1002/2015GC005750.
10. Zhao, Y.; Tzedakis, P.C.; Li, Q.; Qin, F.; Cui, Q.; Liang, C.; John BBirks, H.; Liu, Y.; Zhang, Z.; Guo, Z.; et al. Evolution of vegetation and climate variability on the Tibetan Plateau over the past 1.74 million years. *Sci. Adv.* **2020**, *6*, eaay6193.
11. Hodell, D.A.; Channell, J.E.T. Mode transitions in Northern Hemisphere glaciation: Co-evolution of millennial and orbital variability in Quaternary climate. *Clim. Past* **2016**, *12*, 1805–1828. https://doi.org/10.5194/cp-12-1805-2016.
12. Guo, Z.T.; Ruddiman, W.F.; Hao, Q.Z.; Wu, H.B.; Qiao, Y.S.; Zhu, R.X.; Peng, S.Z.; Wei, J.J.; Yuan, B.Y.; Liu, T.S.; et al. Onset of Asian desertication by 22 Myr ago inferred from loess deposits in China. *Nature* **2001**, *416*, 159–163.
13. Poulton, S.W.; Canfield, D.E. Development of a sequential extraction procedure for iron: Implications for iron partitioning in continentally derived particulates. *Chem. Geol.* **2005**, *214*, 209–221. https://doi.org/10.1016/j.chemgeo.2004.09.003.
14. Li, C.; Love, G.D.; Lyons, T.W.; Fike, D.A.; Sessions, A.L.; Chu, X. A stratified redox model for the Ediacaran ocean. *Science* **2010**, *328*, 80–83. https://doi.org/10.1126/science.1182369.
15. Fu, Y.; Hao, Q.; Peng, S.; Markovic, S.B.; Gao, X.; Han, L.; Wu, X.; Namier, N.; Zhang, W.; Gavrilov, M.B.; et al. Clay Mineralogy of The Stari Slankamen (Serbia) Loess-Paleosol Sequence During The Last Glacial Cycle—Implications For Dust Provenance and Interglacial Climate. *Quat. Sci. Rev.* **2021**, *263*, 106990. https://doi.org/10.1016/j.quascirev.2021.106990.
16. Lu, H.; An, Z. The Research of The Effect of Different Pretreatments to The Particle Size Measurement of Loess. *Chin. Sci. Bull.* **1997**, *42*, 2535–2538.
17. Longstaffe, F.J. Oxygen Isotope Studies of Diagenesis and Pore-water Evolution in The Basal Belly River Sandstone, Pembina I.-poor, Alberta. *J. Sediment. Res.* **1986**, *58*, 489–505.
18. Ayalon, A.; Longstaffe, F.J. Isolation of Diagenetic Silicate Minerals in Clastic Sedimentary Rocks for Oxygen Isotope Analysis; A summary of Methods. *Isr. J. Earth-Sci.* **1992**, *38*, 139–148.
19. Vuković, Z.; Milutonović, A.; Rožić, L.; Rosić, A.; Nedić, Z.; Jovanović, D. The Influence of Acid Treatment on The Composition of Bentonite. *Clays Clay Miner.* **2006**, *54*, 697–702. https://doi.org/10.1346/CCMN.2006.0540605.
20. Wallis, P.J.; Gates, W.P.; Patti, A.F.; Scott, J.L.; Teoh, E. Assessing and Improving the Catalytic Activity of K-10 Montmorillonite. *Green Chem.* **2007**, *9*, 980–986. https://doi.org/10.1039/b701504f.
21. Jiang, J.; Feng, L.; Gu, X.; Qian, Y.; Gu, Y.; Duanmu, C. Synthesis of Zeolite A From Palygorskite Via Acid Activation. *Appl. Clay Sci.* **2012**, *55*, 108–113. https://doi.org/10.1016/j.clay.2011.10.014.
22. Komadel, P. Acid Activated Clays: Materials in Continuous Demand. *Appl. Clay Sci.* **2016**, *131*, 84–99. https://doi.org/10.1016/j.clay.2016.05.001.
23. Zhang, C.; Paterson, G.A.; Liu, Q. A new mechanism for the magnetic enhancement of hematite during heating: The role of clay minerals. *Stud. Geophys. Geod.* **2011**, *56*, 845–860. https://doi.org/10.1007/s11200-011-9018-4.
24. Lv, Y.; Zhang, C.; Fu, Y.; Wu, H.; Hao, Q.; Qiao, Y.; Guo, Z. Clay mineralogical and geochemical record from a loess-paleosol sequence in Chinese Loess Plateau during the past 880 ka and the implication on the East Asian Summer Monsoon. *Quat. Sci.* **2022**, *42*, 921–938. https://doi.org/10.11928/j.issn.1001-7410.2022.04.01.
25. Kahle, M.; Kleber, M.; Jahn, R. Review of XRD-based quantitative analyses of clay minerals in soils: The suitability of mineral intensity factors. *Geoderma* **2002**, *109*, 191–205.
26. Biscaye, P.E. Mineralogy and Sedimentation of Recent Deep-Sea Clay in the Atlantic Ocean and Adjacent Seas and Oceans. *Geol. Soc. Am. Bull.* **1965**, *76*, 803–832.

27. Zhou, X.; Liu, D.; Bu, H.; Deng, L.; Liu, H.; Yuan, P.; Du, P.; Song, H. XRD-based quantitative analysis of clay minerals using reference intensity ratios, mineral intensity factors, Rietveld, and full pattern summation methods: A critical review. *Solid Earth Sci.* **2018**, *3*, 16–29. https://doi.org/10.1016/j.sesci.2017.12.002.
28. Hillier, S. Quantitative Analysis of Clay and other Minerals in Sandstones by X-Ray Powder Diffraction (XRPD). *Clay Miner. Cem. Sandstones* **1999**, 213–251, doi:https://doi.org/10.1002/9781444304336.ch11.
29. Barzegar, A.R.; Oades, J.M.; Rengasamy, P.; Murray, R.S. Tensile strength of dry, remoulded soils as affected by properties of the clay fraction. *Geoderma* **1995**, *65*, 93–108. https://doi.org/10.1016/0016-7061(94)00028-9.
30. Ransom, B.; Kim, D.; Kastner, M.; Wainwright, S. Organic matter preservation on continental slopes: Importance of mineralogy and surface area. *Geochim. Cosmochim. Acta* **1998**, *62*, 1329–1345. https://doi.org/10.1016/S0016-7037(98)00050-7.
31. Liu, Z.; Colin, C.; Li, X.; Zhao, Y.; Tuo, S.; Chen, Z.; Siringan, F.P.; Liu, J.T.; Huang, C.; You, C.; et al. Clay mineral distribution in surface sediments of the northeastern South China Sea and surrounding fluvial drainage basins: Source and transport. *Mar. Geol.* **2010**, *277*, 48–60. https://doi.org/10.1016/j.margeo.2010.08.010.
32. Li, P.; Zhang, C.; Kelley, J.; Deng, C.; Ji, X.; Jablonski, N.G.; Wu, H.; Fu, Y.; Guo, Z.; Zhu, R. Late Miocene Climate Cooling Contributed to the Disappearance of Hominoids in Yunnan Region, Southwestern China. *Geophys. Res. Lett.* **2020**, *47*, e2020GL087741. https://doi.org/10.1029/2020GL087741.
33. Petschick, R. MacDiff 4.2.2. 2000. Available online: http://mill2.chem.ucl.ac.uk/ccp/web-mirrors/krumm/macsoftware/macdiff/MacDiff.html (accessed on 8 August 2022)
34. Steudel, A.; Batenburg, L.F.; Fischer, H.R.; Weidler, P.G.; Emmerich, K. Alteration of swelling clay minerals by acid activation. *Appl. Clay Sci.* **2009**, *44*, 105–115. https://doi.org/10.1016/j.clay.2009.02.002.
35. Tkáč, I.; Komadel, P.; Müller, D. Acid-Treated Montmorillonites—A Study by 29Si and 27Al MAS NMR. *Clay Miner.* **1994**, *29*, 11–19.
36. Novák, I.; Číčel, B. Dissolution of Smectites in Hydrochloric Acid: II. Dissolution Rate as A Function of Crystallochemical Composition. *Clays Clay Miner.* **1978**, *26*, 341–344.
37. Bailey, S.W. *Structures of Layer Silicates and Their X-ray Identification*; Brown, G., Brindley, G.W., Eds.; Mineralogical Society: London, UK, 1980.
38. Steudel, A.; Batenburg, L.F.; Fischer, H.R.; Weidler, P.G.; Emmerich, K. Alteration of non-swelling clay minerals and magadiite by acid activation. *Appl. Clay Sci.* **2009**, *44*, 95–104. https://doi.org/10.1016/j.clay.2009.02.001.
39. Gajam, S.Y.; Raghavan, S. A Kinetic Model for the H Acid Leaching of Kaolinite Clay in the Presence of Fluoride Ions. *Hydrometallurgy* **1985**, *15*, 143–158. https://doi.org/10.1016/0304-386X(85)90050-7.
40. Escamilla-Roa, E.; Nieto, F.; Sainz-Díaz, C.I. Stability of the Hydronium Cation in the Structure of Illite. *Clays Clay Miner.* **2016**, *64*, 413–424. https://doi.org/10.1346/CCMN.2016.0640406.
41. Bloss, F.D. *Crystallography and Crystal Chemistry: An Introduction*; Mineralogical Society of America: Washington, DC, USA, 1994.
42. Zhang, N.X.; Li, Y.; Zhao, H.; Ji, S. *The Research Methods of Clay Mineral*; China Science Publishing & Media LTD: Beijing, China, 1990.
43. Velde, B.; Meunier, A. *The Origin of Clay Minerals in Soils and Weathered Rocks*; Springer: Berlin/Heidelberg, Germany; New York, NY, USA, 2008.
44. Fagel, N. Clay Minerals, Deep Circulation and Climate. *Dev. Mar. Geol.* **2007**, *1*, 139–184, doi:https://doi.org/10.1016/S1572-5480(07)01009-3
45. Chamley, H. *Clay Sedimentology*; Springer: Berlin/Heidelberg, Germany, 1989.
46. Bao, H.; Koch, P.L.; Rumble, D.I. Paleocene–Eocene Climatic Variation in Western North America: Evidence From The Δ18O of Pedogenic Hematite. *GSA Bull.* **1999**, *111*, 1405–1415. https://doi.org/10.1130/0016-7606(1999)111<1405:PECVIW>2.3.CO;2.